

## Observations of sheared turbulence in the H-mode $E_r$ well by phase contrast imaging on DIII-D

J.C. Rost<sup>1</sup>, A. Marinoni<sup>1</sup>, E.M. Davis<sup>1</sup>, M. Porkolab<sup>1</sup>, K.H. Burrell<sup>2</sup>

<sup>1</sup> Massachusetts Institute of Technology, Cambridge, USA

<sup>2</sup> General Atomics, San Diego, USA

Phase Contrast Imaging (PCI) has been used on DIII-D to measure turbulent density fluctuations in several H-mode regimes, observing highly sheared turbulence in the  $E_r$  well. Turbulence at moderate frequencies  $f < 600$  kHz is seen in the pedestal and extends into the  $E_r$  well where eddies are distorted by sheared flow. Turbulence at high frequencies  $f > 800$  kHz is seen at the center of the  $E_r$  well propagating in the lab frame at the highest  $\mathbf{E} \times \mathbf{B}$  velocity in the edge.

### Background

PCI is a line-integrated scattering diagnostic which images electron density turbulence onto a detector array, with flat response in the range  $1 < k < 25$  cm<sup>-1</sup> in the DIII-D implementation, corresponding roughly to  $0.2 < k\rho_s < 5$ . [1, 2] The spectrum of broadband turbulence has a finite spread in  $(k_r, k_\theta)$  space, and the PCI response selects the component of the spectrum which is perpendicular to the roughly vertical laser beam (see Fig. 1). Shear in the  $\mathbf{E} \times \mathbf{B}$  velocity has the effects of, first, decreasing the radial correlation length, hence increasing the spectral width  $\Delta k_r = 2/L_r$ , and second shifting the turbulence to finite radial wavenumber [3].

A typical spectrum in ELM-free H-mode as in Fig. 2 shows multiple turbulent modes from different locations along the beampath, distinguished by their lab-frame phase velocities. The “medium frequency” mode is described by  $100 < f < 600$  kHz and lab-frame phase velocity  $10 < v_{ph} < 20$  km/s, typical  $\mathbf{E} \times \mathbf{B}$  velocities near the top of the pedestal. The “high frequency” mode,  $800$  kHz  $< f < 2$  MHz, lies in the range  $30 < v_{ph} < 80$  km/s, similar to  $V_{\mathbf{E} \times \mathbf{B}}$  at the center of the  $E_r$  well. The two ranges of turbulence show similar behavior across many H-mode regimes, including ELM-free, ELM<sub>y</sub>, and QH-mode. Of these, only QH-mode discharges provide measurements in stationary or slowly-varying plasmas and are hence most amenable to study.

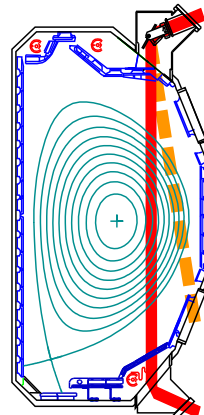


Figure 1: DIII-D cross section showing core PCI beampath in red and edge beampath as orange dashed line.

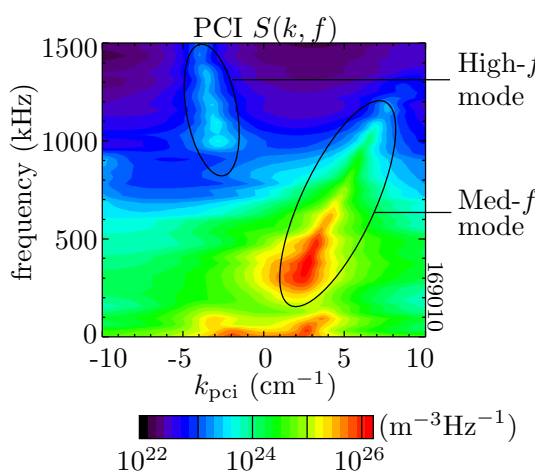


Figure 2: Typical H-mode PCI spectrum  $S(k, f)$  showing medium and high frequency turbulence.

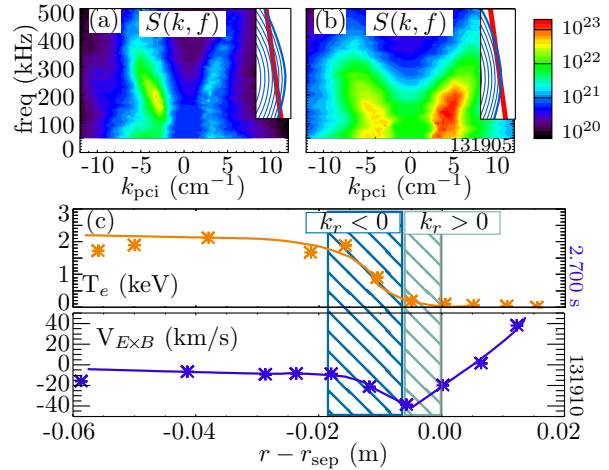


Figure 3: Outer gap scan moved PCI beam from interior path (a) to extreme plasma edge (b), allowing determination of sheared turbulence location (c) with respect to electron temperature pedestal and  $E_r$  well.

### H-mode turbulence in the medium frequency range

Studies of this turbulence using both beampaths in Fig. 1 suggest that the turbulence is driven near the top of the pedestal and extends into the  $E_r$  well. As described below, measurements with the core beampath (red line in Fig. 1) are sensitive to sheared turbulence with  $k_r \sim k_\theta$  and show a lab-frame phase velocity  $v_{ph}$  tied to the  $V_{E \times B}$  at the top of the pedestal. Measurements with the edge beampath (orange dashed line in Fig. 1) are sensitive to *highly* sheared turbulence with  $k_r \sim 2k_\theta$  and record turbulence localized to the  $E_r$  well and sensitive to well parameters.

Scans of the plasma separatrix location in QH-mode [4] with stationary parameters moved the turbulence through the PCI edge beampath, allowing the radial structure to be directly measured, showing that this highly-sheared turbulence was situated in the  $E_r$  well [3], in the location shown in Fig. 3. Modeling the fluctuations as fully-developed turbulence with constant parameters shows that the measurements represent turbulence with  $k_r > 0$  in the outer half of the  $E_r$  well and  $k_r < 0$  on the inner half, as expected from the sign of the shear.

In the core PCI beam location (red line in Fig. 1) the PCI is sensitive to turbulence less distorted by shear, and observations of medium frequency turbulence show that the lab-frame phase velocity is similar to  $V_{E \times B}$  at the top of the pedestal. This was seen directly during a ramp of the injected beam torque in stationary QH-mode [5] where the counter-current torque is decreased from 4 N·m to -1 N·m, causing the  $E \times B$  velocity at 3 cm inside the separatrix near the top of the pedestal to go from 15 km/s ( $e^-$  direction) to -5 km/s as shown in Fig. 4. The turbulence phase velocity is seen to follow this exactly, including reversing sign. This suggests that the turbulent instability is driven near the top of the pedestal.

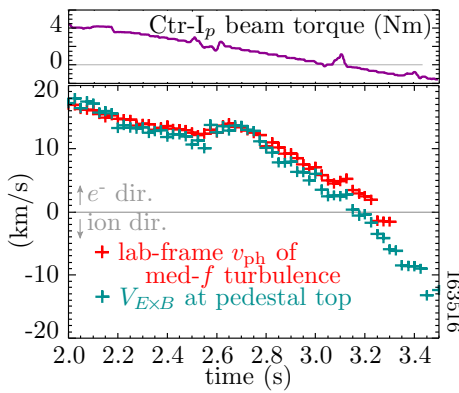


Figure 4: H-mode turbulence lab-frame phase velocity tracks  $\mathbf{E} \times \mathbf{B}$  velocity at the top of the pedestal.

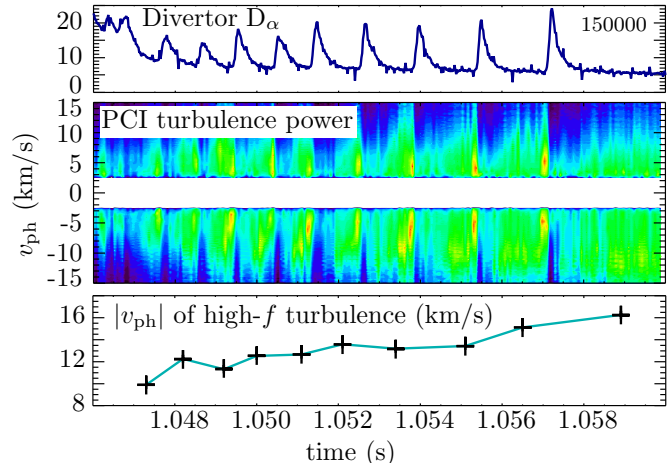


Figure 5: High frequency turbulence allows fast diagnosis of  $E_r$  well in limit-cycle oscillations.

### High frequency instability in the center of the $E_r$ well

In various H-mode regimes the PCI observes high-frequency broadband turbulence  $800 \text{ kHz} < f < 2 \text{ MHz}$  with typical wavenumbers  $1 < k_{\text{pci}} < 4 \text{ cm}^{-1}$ . The turbulence propagates with a well-defined  $v_{\text{ph}}$  with a value in the range  $30 < v_{\text{ph}} < 80 \text{ km/s}$  which is always similar to the  $V_{\mathbf{E} \times \mathbf{B}}$  at the center of the  $E_r$  well.

There are two timescales to  $E_r$  well formation at the H-mode transition. The deep center of the well forms on sub-ms times scales [6] and does not evolve further, while  $E_r$  farther inside the plasma and the pedestal profiles evolve for 10s or 100s of ms. The high-frequency turbulence arises faster than  $100 \mu\text{s}$ , and  $v_{\text{ph}}$  does not evolve with the pedestal parameters, indicating a dependence on the fast-forming center of the well. The high-frequency turbulence can thus be used as an  $E_r$  well diagnostic with higher time resolution than is typically available from direct flow measurements. For example, during Limit Cycle Oscillations (LCO) [7] the  $E_r$  well forms and collapses repeatedly with a cycle on the order of 1 ms. The PCI spectra calculated every  $60 \mu\text{s}$  can resolve the portion of each LCO cycle in which the  $E_r$  well has formed and thereby determine that the well is deeper each cycle until it attains full H-mode depth and the plasma transitions from the LCO to H-mode as seen in Fig. 5.

The high-frequency turbulence is never seen in high-torque QH-mode. It is speculated that the well becomes too narrow to support the instability. However, at lower levels of beam torque injection, the QH-mode transitions to wider edge profiles and a wider, less deep  $E_r$  well, called wide-pedestal QH-mode [5], where the high-frequency turbulence is observed. As the input torque is decreased, the depth of the  $E_r$  well also decreases, and the turbulence  $v_{\text{ph}}$  is seen to track  $V_{\mathbf{E} \times \mathbf{B}}$  at the center of the well with a small intrinsic phase velocity.

## Conclusions

Phase Contrast Imaging observes highly-sheared turbulence in the edge of various H-mode regimes. Medium frequency fluctuations are situated at the top of the pedestal and extend radially into the  $E_r$  well where the turbulence has large  $k_r$  and short correlation lengths. The high-frequency range is driven in the center of the  $E_r$  well and provides a high-time-resolution indirect diagnosis of the evolution of the  $E_r$  well.

Though the pedestal in ELMing H-modes is well predicted by current theories [8], the pedestal in non-ELMing regimes sits away from the ELM threshold, and it is not known what role electrostatic turbulent transport may play in accessing or maintaining these regimes. Modeling the pedestal region of the plasma is an area of active research, with the steep gradients challenging both the theory and the numerics. Linear simulations predicting the high frequency turbulence described here are likely to produce results in the near future. Results will be validated by comparison with PCI observations of wavenumber and sensitivity to the shape of the  $E_r$  well. The medium frequency turbulence requires nonlinear simulations to describe the evolution of eddies in large flow shear. Use of the PCI synthetic diagnostic [3] will account for the geometric effects and permit comparison with the observed spatial variation of radial wavenumber.

## Acknowledgments

This material is based upon work supported by the U.S. Department of Energy, Office of Science, Office of Fusion Energy Sciences under Award Numbers DE-FG02-94ER54235, DE-SC0016154, DE-FC02-99ER54512, and DE-FC02-04ER54698. DIII-D data shown in this paper can be obtained in digital format by following the links at [https://fusion.gat.com/global/D3D\\_DMP](https://fusion.gat.com/global/D3D_DMP).

This report was prepared as an account of work sponsored by an agency of the United States Government. Neither the United States Government nor any agency thereof, nor any of their employees, makes any warranty, express or implied, or assumes any legal liability or responsibility for the accuracy, completeness, or usefulness of any information, apparatus, product, or process disclosed, or represents that its use would not infringe privately owned rights. Reference herein to any specific commercial product, process, or service by trade name, trademark, manufacturer, or otherwise does not necessarily constitute or imply its endorsement, recommendation, or favoring by the United States Government or any agency thereof. The views and opinions of authors expressed herein do not necessarily state or reflect those of the United States Government or any agency thereof.

## References

- [1] J. R. Dorris, J. C. Rost, and M. Porkolab. *Rev. Sci. Instrum.*, **80**:023503 (2009).
- [2] E. M. Davis, J. C. Rost, M. Porkolab, et al. *Rev. Sci. Instrum.*, **87**:11E117 (2016).
- [3] J. C. Rost, M. Porkolab, J. Dorris, and K. H. Burrell. *Phys. Plasmas*, **21**:062306 (2014).
- [4] K. H. Burrell, W. P. West, E. J. Doyle, et al. *Phys. Plasmas*, **12**:056121 (2005).
- [5] X. Chen, K. Burrell, T. Osborne, et al. *Nuclear Fusion*, **57**:022007 (2017).
- [6] R. A. Moyer, K. H. Burrell, T. N. Carlstrom, et al. *Phys. Plasmas*, **2**:2397 (1995).
- [7] L. Schmitz. *Nucl. Fusion*, **57**:025003 (2017).
- [8] P. B. Snyder, T. H. Osborne, K. H. Burrell, et al. *Phys. Plasmas*, **19**:056115 (2012).